J Mater Sci (2011) 46:5639–5644
DOI 10.1007/s10853-011-5514-8

The effect of preparation method on the activities of Pd–Fe–Ox/Al_2O_3 catalysts for CO oxidation

Lili Cai · Guanzhong Lu · Wangcheng Zhan · Yun Guo · Yanglong Guo · Qingshan Yang · Zhigang Zhang

Received: 20 October 2010 / Accepted: 29 March 2011 / Published online: 8 April 2011

Abstract The Pd–Fe–Ox/Al_2O_3 catalysts were prepared by co-impregnation (co-Pd–Fe–Ox/Al_2O_3) and sol–gel method (sol–gel–Pd–Fe–Ox/Al_2O_3) and characterized by N_2 adsorption–desorption, X-ray diffraction (XRD), H_2-temperature programmed reduction (H_2-TPR), and X-ray photoelectron spectroscopy (XPS). The CO catalytic oxidation was investigated over Pd–Fe–Ox/Al_2O_3 catalysts prepared by different methods. The 100% conversion temperature (T_{100}) over pre-reduced co-Pd–Fe–Ox/Al_2O_3 (co-Pd–Fe–Ox/Al_2O_3–R) and pre-reduced sol–gel–Pd–Fe–Ox/Al_2O_3 (sol–gel–Pd–Fe–Ox/Al_2O_3–R) is 90 and 25 °C when fed with the reaction mixture containing 1 vol.% CO and a balance of air, respectively. XRD results indicate that the sol–gel method is favorable for the high dispersion of PdO particles compared with co-impregnation method. H_2-TPR results suggest that the interaction between Pd and Fe is existent over both sol–gel–Pd–Fe–Ox/Al_2O_3 and co-Pd–Fe–Ox/Al_2O_3 catalysts, while the interaction in former catalyst is stronger than that in the latter. The XPS results show that the Pd species on the surface of both sol–gel–Pd–Fe–Ox/Al_2O_3–R and co-Pd–Fe–Ox/Al_2O_3–R catalysts are the mixture of oxide and metal state, leading to the high activity for CO oxidation. Furthermore, the different Pd^{2+}/Pd^0 ratio may be the reason for the different activity between sol–gel–Pd–Fe–Ox/Al_2O_3–R and reduced co-Pd–Fe–Ox/Al_2O_3–R catalysts.

L. Cai · G. Lu · W. Zhan (✉) · Y. Guo · Y. Guo · Q. Yang · Z. Zhang (✉)
Lab for Advanced Materials, Research Institute of Industrial Catalysis, East China University of Science and Technology, Shanghai 200237, People's Republic of China
e-mail: zhanwc@ecust.edu.cn

Z. Zhang
e-mail: zhgzhang@ecust.edu.cn

Introduction

Environmental pollutants produced on consumer sites are increasing along with the growth of civilian activities. The catalytic oxidation of CO has attracted considerable attention due to the increasing applications in the automotive emission control, trace CO removal in the enclosed atmospheres, and exhaust abatement in carbon dioxide lasers. Up to now, the catalysts for CO oxidation are mainly focused on noble metals (such as Au, Pt, Pd, etc.) [1–6] supported on reducible or inert oxides and some transition metal oxide catalysts (such as Co, Mn, Fe, Cu, and Ce) [7–12]. It is unfortunate that noble metal catalysts suffer from the high price of noble metal, while transition metal oxide catalysts generally present a low activity. This resulted in vigorous activity surrounding the preparation of catalysts with low amount of noble metal and high activity by introducing a transition metallic component, such as supported Au–(CeOx, CuOx) [13], Pt–(FeOx, CeOx, SnOx) [2, 14–17], and Pd–(CeOx, Fe_2O_3, CrOx) [3, 18, 19]. Generally, the introduction of transition metal can improve the dispersity of noble metal species and the activity [3, 13–19]. For example, the introduction of Fe into the Pd/NaZSM increased the dispersion of the active Pd species and Pd species were easy to enrich on the surface of the Pd–Fe–O/NaZSM catalyst. As a result, the 100% conversion temperatures for CO oxidation decreased from 180 to 47 °C [3]. However, Pd–Fe bimetallic catalysts supported on Al_2O_3 are rarely studied for CO oxidation, besides the hydrogenation of styrene [20] or dienes [21], and the dechlorination of aromatic compounds [22, 23].

In this study, the alumina-supported bimetallic Pd–Fe catalysts were prepared by co-impregnation and sol–gel method, respectively, and characterized by BET, X-ray diffraction (XRD), H_2-temperature programmed reduction

(H_2-TPR), and X-ray photoelectron spectroscopy (XPS). Their catalytic performances for low temperature CO oxidation were studied, and the effect of preparation method on the activities of Pd–Fe–Ox/Al_2O_3 catalysts for CO oxidation was discussed in detail.

Experimental

Preparation of supported Pd–Fe catalysts

Pd–Fe–Ox/Al_2O_3 catalyst was prepared by simultaneous wet impregnation method as follows: the appropriate amounts of aqueous $Pd(NO_3)_2$ and $Fe(NO_3)_3$ were mixed, and then the alumina was added into the mixture. The mass fraction is 1 and 14 wt% for Pd and Fe, respectively. After being stirred at 30 °C for 24 h, the solid was dried at 120 °C for 12 h in air, and calcined at 550 °C for 2 h in air. The sample prepared was designated as co-Pd–Fe–Ox/Al_2O_3.

On the other hand, Pd–Fe–Ox/Al_2O_3 catalyst was prepared by the sol–gel method as follows: the appropriate amounts of aqueous $C_6H_8O_7{\cdot}H_2O$, $Pd(NO_3)_2$, and $Fe(NO_3)_3$ were mixed, and then the alumina was added into the mixture. The mass fraction is 1 and 14 wt% for Pd and Fe, respectively. After being placed for 24 h, the mixed solution was evaporated in water bath at 70 °C until the gel was appeared. Then the gel was moved to oil bath at 150 °C subsequently, and the formed brown mixture was dried at 120 °C for 12 h in air, calcined at 550 °C for 2 h in air. The sample prepared was designated as sol–gel–Pd–Fe–Ox/Al_2O_3.

Pd/Al_2O_3 and Fe/Al_2O_3 catalysts were prepared with the same procedure as sol–gel–Pd–Fe–Ox/Al_2O_3. The prepared catalysts were designated as sol–gel–Pd/Al_2O_3 and sol–gel–Fe/Al_2O_3, respectively.

A series of alumina-supported mono- and bimetallic Pd–Fe catalysts were further reduced with 10 vol.% H_2 (nitrogen balanced) at 90 °C for 30 min. The samples were denoted as co-Pd–Fe–Ox/Al_2O_3–R, sol–gel–Pd–Fe–Ox/Al_2O_3–R, sol–gel–Pd/Al_2O_3–R, and sol–gel–Fe/Al_2O_3–R, respectively.

Characterization of materials

N_2 adsorption–desorption isotherms were measured at 77 K on a NOVA 4000e apparatus. Prior to the measurements, all samples were degassed at 180 °C for 12 h. The special surface area was assessed using the BET method. XRD patterns were recorded on a Bruke FOCUS 8 diffractometer with Cu K_α radiation ($\lambda = 0.154$ nm) at a scanning rate of 6°/min in the 2θ range of 10–80°. XPS data were acquired on a Thermo ESCALAB 250 spectrometer using Al K_α X-ray radiation (1486.6 eV). H_2-TPR was carried out in a quartz microreactor. 50 mg sample was heated up to 800 °C from room temperature at a rate of 10 °C/min in 5 vol.% H_2/N_2 mixture gas with a flow rate of 45 mL/min. The amount of H_2 during the reduction was determined by TCD.

Catalytic activities test

The catalytic activities of the samples for CO oxidation were measured in a fixed-bed quartz tubular reactor. Each time, 200 mg of the catalyst (40–60 mesh) were loaded in the quartz reactor. The temperature of the catalyst bed was monitored and controlled by temperature controllers. The reaction mixture containing 1 vol.% CO and a balance of air or 1 vol.% CO, 4.2 vol.% H_2O, and a balance of air was fed into the catalyst bed at a flow rate of 50 mL/min. The concentrations of CO and CO_2 in the effluent gas were on-line analyzed by a gas chromatograph (molecular sieve 13× column) equipped with a methane reformer.

The stability of the catalysts for CO oxidation was also investigated in a fixed-bed quartz tubular reactor. 200 mg of the catalyst (40–60 mesh) is loaded in the quartz reactor. The reaction mixture containing 1 vol.% CO, 4.2 vol.% H_2O, and a balance of air was fed into the catalyst bed at a flow rate of 50 mL/min.

Results and discussion

The activity for CO oxidation

The activity and the stability for CO oxidation over different Pd–Fe–Ox/Al_2O_3 catalysts prepared with co-impregnation and sol–gel method are shown in Fig. 1. As shown in Fig. 1A, the 100% conversion temperatures for CO oxidation are 100, 170, and 25 °C over sol–gel–Pd/Al_2O_3–R, sol–gel–Fe/Al_2O_3–R, and sol–gel–Pd–Fe–Ox/Al_2O_3–R, respectively. However, the 100% conversion temperatures for CO oxidation are 90 °C over co-Pd–Fe–Ox/Al_2O_3–R. It is obvious that the preparation method exerts distinct influences on the activity of the catalysts. The effect of moisture on the activity of different catalysts is shown in Fig. 1B. The results show that the 100% conversion temperatures for CO oxidation hardly increases for the catalysts containing Pd (a, c, d). However, the activity of sol–gel–Fe/Al_2O_3–R drastically decreases with the addition of 4.2 vol.% H_2O in the reaction mixture. The 10% conversion temperature (T_{10}) over sol–gel–Fe/Al_2O_3–R is up to 220 °C. Furthermore, it is interesting that the different catalysts show a significant difference in the stability, as shown in Fig. 1C. At 80 °C reaction temperature, under the reaction mixture containing 1 vol.% CO,

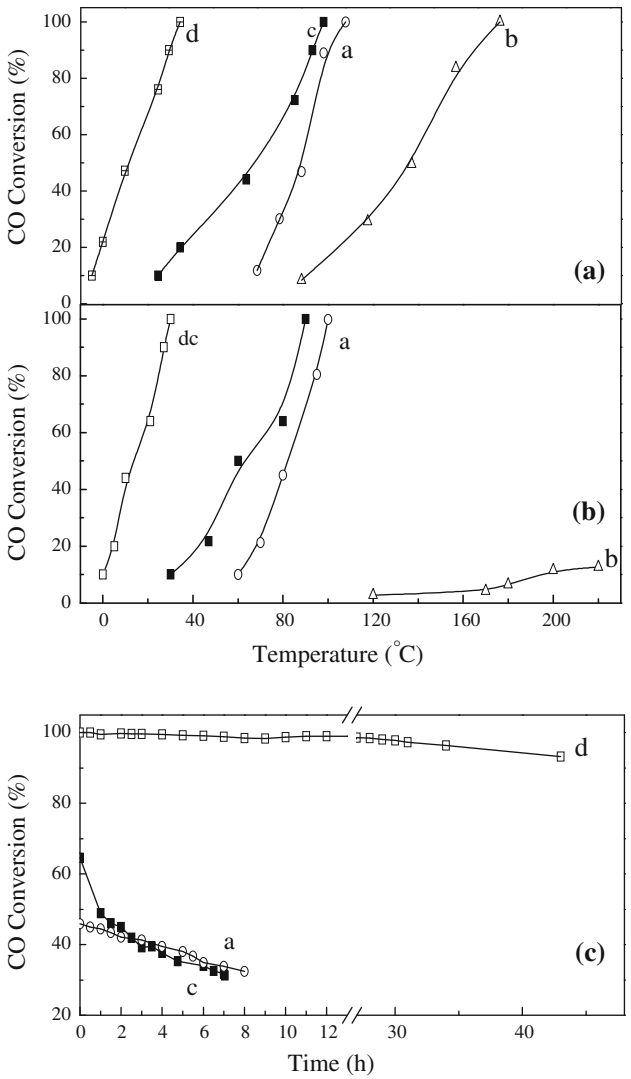

Fig. 1 The activity for CO catalytic oxidation fed with different reaction mixture **A** 1 vol.% CO and a balance of air, **B** 1 vol.% CO, 4.2 vol.% H_2O, and a balance of air, **C** the stability with reaction mixture containing 1 vol.% CO, 4.2 vol.% H_2O, and a balance of air at 80 °C of the catalysts: (*a*) sol–gel–Pd/Al_2O_3–R; (*b*) sol–gel–Fe/Al_2O_3–R; (*c*) co-Pd–Fe–O*x*/Al_2O_3–R; (*d*) sol–gel–Pd–Fe–O*x*/Al_2O_3–R catalysts

4.2 vol.% H_2O, and a balance of air, the activity of sol–gel–Pd–Fe–O*x*/Al_2O_3–R can sustain for about 30 h with nearly 100% CO conversion. With continuously increased the reaction time, the activity of catalyst decreases slightly from 98 to 93% after 43 h reaction. However, the activities of co-Pd–Fe–O*x*/Al_2O_3–R and sol–gel–Pd/Al_2O_3–R catalysts sharply decrease with reaction time. The decrease rate of sol–gel–Pd–Fe–O*x*/Al_2O_3–R activity for CO oxidation is much slower than that of sol–gel–Pd/Al_2O_3–R and co-Pd–Fe–O*x*/Al_2O_3–R, which could demonstrate that the sol–gel–Pd–Fe–O*x*/Al_2O_3–R behaves the highest stability among the tested catalyst. In a word, the preparation method and the introduction of Fe into the catalyst greatly affect the catalytic activity and stability.

Characterization of catalysts

BET

Table 1 shows the physicochemical properties of different catalysts. It is observed that different catalysts display slight difference in the special surface areas, and elemental analysis results show that the catalysts prepared by different methods have the similar loading amount of Pd and Fe. This means that the difference in the activity of different catalysts may be correlated with the state of Pd and Fe in the catalysts, instead of the surface area and the loading amount.

XRD

Figure 2 shows the XRD patterns of the different catalysts. It is clear that all the catalysts display the diffraction peaks of Al_2O_3. As for sol–gel–Pd/Al_2O_3, a diffraction peak appears at $2\theta = 33.84°$, which corresponds to the crystal plane (101) of PdO particles. As for sol–gel–Fe/Al_2O_3, several weak diffraction peaks are observed at $2\theta = 33.41$, 35.74, and 54.04°, which correspond to the crystal plane (104), (110), and (116) of Fe_2O_3, respectively. Although the diffraction peak at $2\theta = 33.84°$ also appears in the XRD profiles of co-Pd–Fe–O*x*/Al_2O_3 and sol–gel–Pd–Fe–O*x*/Al_2O_3 catalysts, the intensity of this peak for the former catalyst is stronger than that for the latter catalyst, which means that the PdO particles are smaller over sol–gel–Pd–Fe–O*x*/Al_2O_3 catalyst than that over co-Pd–Fe–O*x*/Al_2O_3 catalyst. On the other hand, similar with the situation of PdO, the diffraction peaks of Fe_2O_3 are also stronger over the co-Pd–Fe–O*x*/Al_2O_3 catalyst than those over the sol–gel–Pd–Fe–O*x*/Al_2O_3 catalyst. These results indicate that

Table 1 Physicochemical properties of the catalysts

Catalysts	S_{BET} (m^2/g)	EDS (M wt%)[a]		T_{100} (°C)[b]
		Pd	Fe	
sol–gel–Pd–Fe–O*x*/Al_2O_3–R	158	0.61	7.93	25
co-Pd–Fe–O*x*/Al_2O_3–R	170	0.59	8.43	90
sol–gel–Pd/Al_2O_3–R	173	0.69	–	100
sol–gel–Fe/Al_2O_3–R	194	–	8.52	170
Al_2O_3	175	–	–	–

[a] Determined by EDS

[b] The 100% conversion temperature for CO oxidation with 1 vol.% CO/air

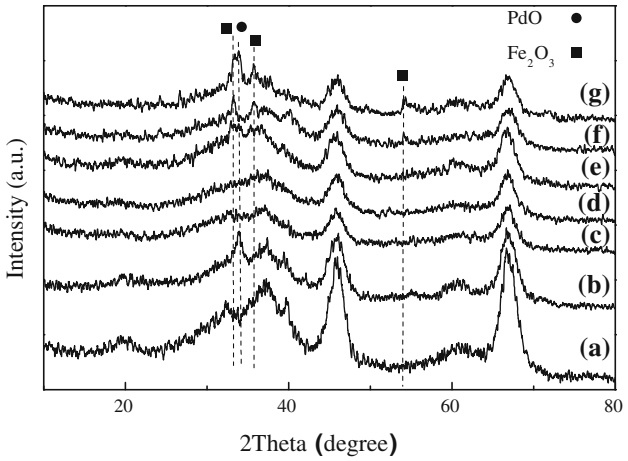

Fig. 2 XRD patterns of different catalysts: (*a*) Al_2O_3, (*b*) sol–gel–Pd/Al_2O_3, (*c*) sol–gel–Fe/Al_2O_3, (*d*) sol–gel–Pd–Fe–O*x*/Al_2O_3–R, (*e*) sol–gel–Pd–Fe–O*x*/Al_2O_3, (*f*) co-Pd–Fe–O*x*/Al_2O_3–R, and (*g*) co-Pd–Fe–O*x*/Al_2O_3

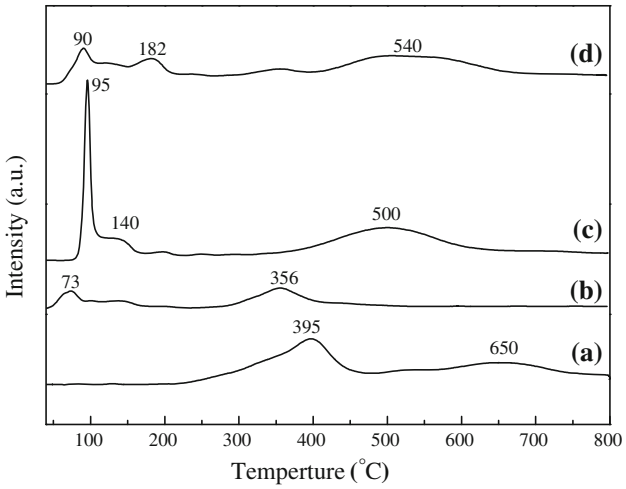

Fig. 3 H_2-TPR profiles of different catalysts: (*a*) sol–gel–Fe/Al_2O_3, (*b*) sol–gel–Pd/Al_2O_3, (*c*) sol–gel–Pd–Fe–O*x*/Al_2O_3, and (*d*) co-Pd–Fe–O*x*/Al_2O_3

the sol–gel method is favorable for the formation of small PdO and Fe_2O_3 particles.

However, the diffraction peaks of PdO and Fe_2O_3 disappear for the sol–gel–Pd–Fe–O*x*/Al_2O_3–R catalyst. As for the co-Pd–Fe–O*x*/Al_2O_3–R, the diffraction peak of PdO disappears and the intensity of the diffraction peaks of Fe_2O_3 becomes weak compared with co-Pd–Fe–O*x*/Al_2O_3 catalyst. These results indicate that the reduction procedure can improve the dispersity of Pd and Fe species, and the dispersity of Pd and Fe species is higher over sol–gel–Pd–Fe–O*x*/Al_2O_3–R catalyst than those over the co-Pd–Fe–O*x*/Al_2O_3–R catalyst. This may be the reason why sol–gel–Pd–Fe–O*x*/Al_2O_3–R and co-Pd–Fe–O*x*/Al_2O_3–R catalysts exhibit the different catalytic performances for CO oxidation.

H_2-TPR

Figure 3 shows the H_2-TPR patterns of unreduced mono- and bimetallic Pd–Fe catalysts. The sol–gel–Fe/Al_2O_3 catalyst shows two reduction peaks with the zenith at 395 and 650 °C, which are attributed to the reduction of Fe^{3+} to Fe^{2+} and Fe^{2+} to Fe^0, respectively [23, 24]. In the light of the reduction peaks of Fe_2O_3 at 487 and 719 °C, it is obvious that the reduction of Fe_2O_3 becomes easy when supported on Al_2O_3, due to the high dispersity of Fe species over the support. As for the catalysts containing Pd, a reduction peak at <100 °C appears which is ascribed to the reduction of Pd^{2+} to Pd^0. However, the areas of this reduction peak are much different among sol–gel–Pd/Al_2O_3, sol–gel–Pd–Fe–O*x*/Al_2O_3, and co-Pd–Fe–O*x*/Al_2O_3 catalysts. Secondly, this reduction peak for sol–gel–Pd–Fe–O*x*/Al_2O_3 and co-Pd–Fe–O*x*/Al_2O_3 catalysts shifts to the high temperature of 95 and 90 °C, compared with the reduction peak at 73 °C for sol–gel–Pd/Al_2O_3. At the same time, the reduction peak of Fe_2O_3 for sol–gel–Pd–Fe–O*x*/Al_2O_3 and co-Pd–Fe–O*x*/Al_2O_3 shifts to the low temperature of 140 and 182 °C, respectively. These results suggest that the addition of Fe into Pd/Al_2O_3 system can improve the stabilization of Pd oxide [3, 23, 24]. In other words, the interaction between Pd and Fe retards the reduction of PdO and facilitates the reduction of Fe_2O_3. Moreover, based on the offset degree of the reduction temperature of PdO and Fe_2O_3, the interaction between Pd and Fe over sol–gel–Pd–Fe–O*x*/Al_2O_3 is stronger than that over co-Pd–Fe–O*x*/Al_2O_3, leading to the high activity of sol–gel–Pd–Fe–O*x*/Al_2O_3–R catalyst for CO oxidation.

XPS

In order to demonstrate active phases of the bimetallic catalysts for CO oxidation in detail, XPS was used to investigate the composition and chemical states of atoms on the surface of different catalysts. The binding energies (BE) of Pd $3d_{5/2}$, Fe $2p_{3/2}$, and Al $2p$, and the surface atomic ratios for the sol–gel–Pd–Fe–O*x*/Al_2O_3–R and co-Pd–Fe–O*x*/Al_2O_3–R catalysts are summarized in Table 2.

It is well known that the surface atom ratio is closely correlated to the dispersity of corresponding metal. The higher surface atom ratio is, the higher is the dispersion [25]. Compared with co-Pd–Fe–O*x*/Al_2O_3–R catalyst, the Pd/Al atomic ratio on the surface of sol–gel–Pd–Fe–O*x*/Al_2O_3–R catalyst is slightly high, which suggests that the sol–gel method tends to high dispersion of Pd particles, matching the results from XRD.

Figure 4 shows the experimental and fitted Pd $3d$ spectra of sol–gel–Pd–Fe–O*x*/Al_2O_3–R and co-Pd–Fe–O*x*/Al_2O_3–R catalysts. The fitting process was referred to in the

Table 2 Surface charaterization results from XPS test

Catalysts	Pd $3d_{5/2}$		Fe $2p_{3/2}$		Al $2p$		Pd/Al [at]/[at]
	BE, eV	[at], %	BE, eV	[at], %	BE, eV	[at], %	
sol–gel–Pd–Fe–Ox/Al_2O_3–R	337.80	0.19	711.59	2.16	74.29	18.85	0.0101
co-Pd–Fe–Ox/Al_2O_3–R	337.83	0.16	711.57	2.45	74.26	18.17	0.0088

literature [26]. It is interesting that both Pd^{2+} and Pd^0 are present on the surface of two catalysts, and Pd^{2+}/Pd^0 ratio on the surface of sol–gel–Pd–Fe–Ox/Al_2O_3–R catalyst is higher than the value on the surface of co-Pd–Fe–Ox/Al_2O_3–R catalyst. As shown in H_2-TPR, the interaction between Pd and Fe can inhibit the reduction of PdO and this interaction over sol–gel–Pd–Fe–Ox/Al_2O_3 catalyst is stronger than that over co-Pd–Fe–Ox/Al_2O_3 catalyst, leading to the high Pd^{2+}/Pd^0 ratio over sol–gel–Pd–Fe–Ox/Al_2O_3–R catalyst.

The XPS spectra show that the Pd species are the mixture of oxide and metal state on the surface of both sol–gel–Pd–Fe–Ox/Al_2O_3–R and co-Pd–Fe–Ox/Al_2O_3–R catalysts, which is in compliance with the "metal ion-metal nanoclusters" model [2, 4, 27, 28], leading to the high activity of both catalysts for CO oxidation. On the other hand, the optimum Pd^{2+}/Pd^0 value may be existent for the highest activity of CO oxidation. In our experiment, the effect of the reduction temperature on the activity of sol–gel–Pd–Fe–Ox/Al_2O_3 catalyst has been studied and the results are shown in Table 3. The results reveal that the reduction at different temperature, corresponding to the different Pd^{2+}/Pd^0 ratio, largely influences the activity of the catalyst. Thus, compared with co-Pd–Fe–Ox/Al_2O_3–R catalyst, the high activity of sol–gel–Pd–Fe–Ox/Al_2O_3–R for CO oxidation may be due to the appropriate Pd^{2+}/Pd^0 ratio.

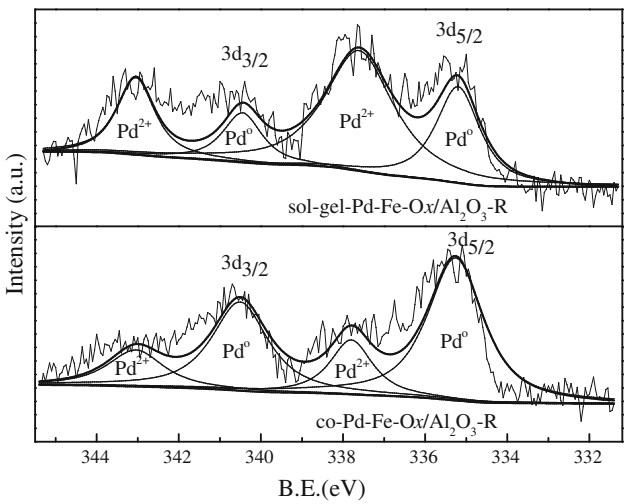

Fig. 4 Pd 3*d* XPS spectra of sol–gel–Pd–Fe–Ox/Al_2O_3–R and co-Pd–Fe–Ox/Al_2O_3–R catalysts

Table 3 The effect of the reduction temperature on the activity of the sol–gel–Pd–Fe–Ox/Al_2O_3–R catalyst

$T_{reduction}$/°C[a]	70	90	100	115	500	650
T_{100}/°C[b]	45	25	50	60	110	120

[a] The reduction temperature of the sol–gel–Pd–Fe–Ox/Al_2O_3–R catalyst

[b] The 100% conversion temperature for CO oxidation with 1 vol.% CO/Air

Conclusions

In this study, the Pd–Fe–Ox/Al_2O_3 catalysts were prepared by co-impregnation (co-Pd–Fe–Ox/Al_2O_3) and sol–gel method (sol–gel–Pd–Fe–Ox/Al_2O_3) and CO catalytic oxidation was investigated over Pd–Fe–Ox/Al_2O_3 catalysts. The 100% conversion temperatures (T_{100}) is 90 and 25 °C for pre-reduced co-Pd–Fe–Ox/Al_2O_3 and pre-reduced sol–gel–Pd–Fe–Ox/Al_2O_3 catalysts with the reaction mixture containing 1 vol.% CO and a balance of air, respectively. XRD, H_2-TPR, and XPS results indicate that the preparation method largely influences the dispersity of PdO particles, the strong interaction between Pd and Fe, and Pd^{2+}/Pd^0 ratio, leading to the different activity of the catalysts for CO oxidation.

Acknowledgements This project was supported financially by National Basic Research Program of China (2010CB732300), National Key Technologies R & D Program of China (2007BAJ03B01), Education Commission of Shanghai Municipality (2008CG35), Science and Technology Commission of Shanghai Municipality (09ZR1408200).

References

1. Cutrufello MG, Rombi E, Cannas C, Casu M, Virga A, Fiorilli S, Onida B, Ferino I (2009) J Mater Sci 44:6644. doi:10.1007/s10853-009-3510-z
2. Margitfalvi JL, Borbáth I, Hegedús M, Tfirst E, Góbölös S, Lázár K (2000) J Catal 196:200
3. Bi YS, Chen L, Lu GX (2007) J Mol Catal A 266:173
4. Qiao BT, Liu LQ, Zhang J, Deng YQ (2009) J Catal 261:241
5. Shen YX, Lu GZ, Guo Y, Wang YQ (2010) Chem Commun 46:8433
6. Liu LQ, Zhou F, Wang LG, Qi XJ, Shi F, Deng YQ (2010) J Catal 274:1
7. Yu YB, Takei T, Ohashi H, He H, Zhang XL, Haruta M (2009) J Catal 267:121
8. Iablokov V, Frey K, Geszti O, Kruse N (2010) Catal Lett 134:210

9. Lin HY, Chen YW, Wang WJ (2005) J Nanopart Res 7:249
10. Cao JL, Shao GS, Ma TY, Wang Y, Ren TZ, Wu SH, Yuan ZY (2009) J Mater Sci 44:6717. doi:10.1007/s10853-009-3583-8
11. Liu Y, Wen C, Guo Y, Lu GZ, Wang YQ (2010) J Mol Catal A 316:59
12. Cao JL, Deng QF, Yuan ZY (2009) J Mater Sci 44:6663. doi: 10.1007/s10853-009-3582-9
13. Lin SD, Gluhoi AC, Nieuwenhuys BE (2004) Catal Today 90:3
14. Liu XS, Korotkikh O, Farrauto R (2002) Appl Catal A 226:293
15. Sirijaruphan A, Goodwin JG Jr, Rice RW (2004) J Catal 224:304
16. Son IH, Lane AM (2001) Catal Lett 76:151
17. Profeti LPR, Ticianelli EA, Assaf EM (2008) Fuel 87:2076
18. García MF, Arias AM, Yuez AI, Hungría AB, Anderson JA, Conesa JC, Soria J (2003) J Catal 214:220
19. Ciuparu D, Bensalem A, Pfefferle L (2000) Appl Catal B 26:241
20. Pârvulescu VI, Filoti G, Pârvulescu V, Grecu N, Angelescu E, Nicolescu LV (1994) J Mol Catal 89:267
21. Bachir R, Marecot P, Didillon B, Barbier J (1997) Appl Catal A 164:313
22. Nagpal V, Bokara AD, Chikate RC, Rode CV, Paknikar KM (2010) J Hazard Mater 175:680
23. Babu NS, Lingaiah N, Kumar JV, Sai Prasad PS (2009) Appl Catal A 367:70
24. Berry FJ, X CH, Jobson S (1990) J Chem Soc Faraday Trans 86:165
25. Yue BH, Zhou RX, Zheng XM, Lu WC (2008) Fuel Process Technol 89:728
26. Moulder JF, Stickle WF, Esoble PE, Bomben KD (1995) Handbook of X-ray photoelectron spectroscopy. Physical Electronics Inc., USA
27. Guzman J, Gates BC (2004) J Am Chem Soc 126:2672
28. Szegedi A, Hegedus M, Margitfalvi JL, Kiricsi I (2005) Chem Commun 11:1441